

DEVELOPMENT OF AN UNSTEADY AERODYNAMICS MODEL  
TO IMPROVE CORRELATION OF COMPUTED BLADE  
STRESSES WITH TEST DATA

Santu T. Gangwani  
Senior Engineer  
Hughes Helicopters, Inc.  
Culver City, California

Abstract

A reliable rotor aeroelastic analysis operational at Hughes Helicopters, Inc. that correctly predicts the vibration levels for a helicopter is utilized for the present study to test various unsteady aerodynamics models with the objective of improving the correlation between test and theory. This analysis called Rotor Aeroelastic Vibration (RAVIB) computer program is based on a frequency domain forced response analysis which utilizes the transfer matrix techniques to model helicopter/rotor dynamic systems of varying degrees of complexity. The analysis is a non-modal analysis and it includes effects of periodic coefficients for the forward flight conditions. The first new aerodynamics model incorporated in the analysis was based on the current state-of-art of unsteady aerodynamics. The results based on this aerodynamics model for the AH-1G helicopter rotor were compared with the flight test data during high speed operation and they indicated a reasonably good correlation for the beamwise and chordwise blade bending moments, but for torsional moments the correlation was poor. As a result, a new aerodynamics model based on unstalled synthesized data derived from the large amplitude oscillating airfoil experiments was developed and tested with RAVIB analysis. The results indicate a significant improvement in the correlation for the torsional moments.

Introduction

The rotor aeroelastic stability and response analyses (e.g., Reference 1) invariably involve computation of airloads through use of unsteady strip theories. To a significant extent, accuracy of analytically predicted parameters, such as aerodynamic damping, blade oscillatory bending and torsional moments and hub vibratory loads, depends on the correctness of the unsteady aerodynamics model utilized in the analysis. Recently there has been significant effort (References 2-5) to develop new unsteady aerodynamics models for the rotary-wing applications with a correct emphasis on incorporation of precise nature of wind and rotor blade motions. But it has not been fully demonstrated (through correlation with test data) the kind of improvements we can expect by utilizing these more sophisticated unsteady aerodynamic models. The present study was undertaken to test various unsteady aerodynamics models with the primary objective of improving the correlation between the flight test data and theory.

Background

Most of the unsteady aerodynamics models involve extension of Theoderson's flat plate

Presented at the 2nd Decennial Specialists' Meeting on Rotorcraft Dynamics, Ames Research Center, California, November 1984.

theory (Reference 6) to account for the airfoil pitch-plunge motion and also to represent the effects of time-varying free stream velocity. The airfoil shape and thickness effects are normally accounted through replacement of the flat plate lift curve slope ( $2\pi$ ) by an appropriate airfoil static lift curve slope. Blade section unsteady lift and pitching moment coefficients normally involve a lift deficiency function  $C'(k)$ ; where  $k$  is the reduced frequency. For rotary wing applications, where blade section experiences arbitrary motions, use of reduced frequency is highly inappropriate. Therefore, in rotor aeroelastic analyses, it is practical to model unsteady aerodynamics of airfoil arbitrary motions preferably in both Laplace and time domains. This is simply achieved by converting the generalized lift deficiency function into Pade' form (e.g., Reference 7) where it is directly available in Laplace domain. For the time-domain applications, Pade' form can be easily converted into highly practical indicial formulations, such as indicial form of Wagner function for the oscillating flat plate.

Despite availability of the above-mentioned methodology for unsteady strip theory, most of the rotary-wing dynamicists find it convenient to just replace the lift deficiency function by a constant number. Conventionally a value of 0.8 to 1.0 for  $C'(k)$  is used. To date, an uncertainty exists regarding the benefits of these more sophisticated unsteady aerodynamics theories. However, the present study clearly indicates that conventional aerodynamics models are highly inaccurate in predicting certain blade section airloads, such as unsteady pitching moment. More specifically, a new but conventional unsteady aerodynamics model (including aerodynamic spring-damper matrices) based on current state-of-art of the rotary-wing aerodynamics (Reference 8) was developed and it was incorporated into a reliable rotor aeroelastic analysis operational at Hughes Helicopters, Inc. (Reference 1). The computed results (airloads and oscillatory blade bending and torsional moments) for AH-1G rotor blade were compared with the available flight test data corresponding to high speed flight conditions. The correlations obtained for the beamwise and chordwise bending moments were good but for torsional moments, the correlation was poor. As a result, a new unsteady aerodynamics model based on unstalled oscillating airfoil test data was developed and incorporated in the analysis. The results indicate a significant improvement in the correlation of computed oscillatory torsional moments with test data.

Description of Aeroelastic Analysis

The aeroelastic analysis utilized for the present study is called RAVIB (Rotor Aeroelastic Vibration) computer program and it is a modified and improved version of a computer program (References 1 and 9) originally developed by Rochester Applied Science Associates. Briefly,

the RAVIB computer program is based on a frequency domain forced response analysis which utilizes the transfer matrix techniques to model helicopter/rotor dynamic systems of varying degrees of complexity. The analysis is a non-model analysis and it involves application of a standard matrix process in which the transfer matrices associated with successive characteristics of the modeled blade are combined to form the transfer or associate matrix relating the shears, moments, slopes, and deflections at a position on the blade to those occurring at the tip of the blade. The blade mass and structure characteristics are represented in a lumped parameter form. The analysis includes aerodynamic interharmonic blade coupling (periodic coefficients) and interharmonic coupling due to fuselage motion. Only a few features of the analysis will be briefly discussed here. More details are given in Reference 1. Briefly, rotor/helicopter model consists of a rotor system with flexible blades which may be articulated, gimbaled, teetering or hingeless type. The rotor may be connected to fuselage through a fixed system rotor support consisting of gearbox with roll and pitch flexibility and a flexible drive shaft. Fuselage may be modeled as a flexible beam (similar to blade model but non-rotating) or fuselage effects may be represented by a hub impedance matrices. The program has capability to model a detailed swashplate-type control system. The basic rotor blade structure is represented by a lumped parameter model in which the blade is subdivided into a finite number of blade sections. Each blade section may have (see Fig. 1) arbitrary orientation and chordwise location of shear center, arbitrary spanwise distribution of mass and inertias, twist, chord, mass C.G. location, bending and torsional stiffnesses, chordwise aerodynamic center location. The aerodynamic effects include aerodynamic inertia, damping and spring rates which vary azimuthally (periodic coefficients) in forward flight. Radial and azimuthal variations of wake induced velocities may be included. Also, deformed free-wake effects on helicopter rotor system dynamic response may be included in the analysis in an iterative procedure which couples RASA free-wake analysis (Reference 10) to the blade motions.

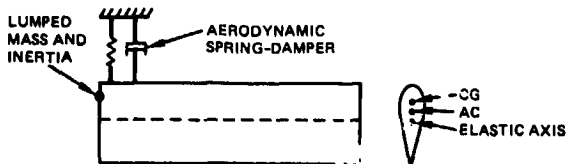


Fig. 1 General blade section model

#### Recent Improvements

As mentioned earlier, the RAVIB analysis has been developed by modifying an existing analysis developed by Rochester Applied Science Associates (Reference 1). A number of these modifications or improvements were absolutely necessary for obtaining a good correlation between predicted results and test data. A few other modifications were carried out to enhance its capabilities.

Most significant of these modifications are listed below:

- 1) An iterative procedure was incorporated in the analysis to obtain the compatible steady state elastic deflections of the blade. A number of sources of blade vibratory excitations (for example, blade aerodynamic pitching moment) vary in a highly nonlinear fashion with the steady state elastic deflection of the blade. Inclusion of this procedure successfully minimizes the error due to these nonlinearities.
- 2) The RAVIB analysis was modified to couple the blade root motions with fuselage through a hub impedance matrix and thus to account for the fuselage motion effects. It is assumed the impedance matrix can be conveniently obtained by exercising NASTRAN.
- 3) Unsteady aerodynamic effects of higher harmonic control (HHC) inputs were incorporated in the analysis.
- 4) A new unsteady aerodynamic model based on the current state-of-art aerodynamics was developed and it was successfully incorporated in the analysis. Further discussions of this unsteady aerodynamics model is provided next.

#### Description of Unsteady Aerodynamics Model

The aerodynamic forces acting on a blade section in time-domain, as it goes around azimuth, can be represented in matrix form by the following relationships:

$$\{F_A\} = \{F_{A0}\} + [M_A]\{\dot{q}\} + [C_A]\{\dot{q}\} + [k_A]\{q\} \quad (1)$$

where  $\{F_{A0}\}$  is a six-component vector of aerodynamic forces and moments in an appropriate coordinate system due to all known motions of blade and wind. The matrices  $[M_A]$ ,  $[C_A]$  and  $[k_A]$  represent mass, damping and spring rates respectively due to aerodynamic forces. The vector  $\{q\}$  is a six-component state vector of unknown deflections and rotations. In general, for steady state helicopter flight conditions, the matrices  $[M_A]$ ,  $[C_A]$  and  $[k_A]$  vary periodically around the azimuth. Furthermore, if Theoderson-type unsteady aerodynamics are utilized, these matrices contain lift deficiency function  $C'(k)$  in one form or another. Because it is not possible to precisely describe the reduced frequency  $k$  for the blade section, some approximations are required to evaluate  $C'(k)$  during the computations. The most common approximation involves assuming a constant value of 0.75 to 1.0 for  $C'(k)$ . The other common procedure involves transforming  $C'(k)$  into indicial form (Reference 7) and computing the airloads in time-domain. This procedure is highly practical for computing  $\{F_{A0}\}$ , where time-history of aerodynamic angle of attack is completely known. The most commonly used indicial form for  $C(k)$  is the Wagner functions (Reference 11) derived from the flat plate theory.

#### Frequency Domain Formulation for Airloads

The present study requires development of aerodynamic transfer matrices in Laplace form that can be used in the frequency-domain analysis of Reference 1. Except for a small magnitude terms involving the function  $[1-C'(k)]$ , each of these periodically varying matrices  $[M_A]$ ,  $[C_A]$  and  $[k_A]$  can be expanded in a Fourier series form. For example,

$$\{C_A\} = \sum_{n=-\infty}^{\infty} [C_n] e^{in\Omega t} \quad (2)$$

Similarly, the periodic motion of the blade around the azimuth can be represented as follows:

$$\{q\} = \sum_{k=-\infty}^{\infty} [q_k] e^{ik\Omega t} \quad (3)$$

Thus the aerodynamic forces generated by elastic deflections  $\{F_{Aq}\}$  involve multiplication of two infinite series resulting in interharmonic coupling as follows:

$$\begin{aligned} \{F_{Aq}\} = & \left( \sum_{n=-\infty}^{\infty} [M_n] e^{in\Omega t} \right) \left( \frac{d^2}{dt^2} \sum_{k=-\infty}^{\infty} [q_k] e^{ik\Omega t} \right) \\ & + \left( \sum_{n=-\infty}^{\infty} [C_n] e^{in\Omega t} \right) \left( \frac{d}{dt} \sum_{k=-\infty}^{\infty} [q_k] e^{ik\Omega t} \right) \\ & + \left( \sum_{n=-\infty}^{\infty} [k_n] e^{in\Omega t} \right) \left( \sum_{k=-\infty}^{\infty} [q_k] e^{ik\Omega t} \right) \quad (4) \end{aligned}$$

Thus, due to periodic coefficients, for example during high speed forward flight, a significant amount of interharmonic coupling occurs.

The Laplace transform is used to transform the differential equations into a set of algebraic equations as follows:

$$\begin{aligned} \{F_{Aq}\}_k = & \sum_{n=-\infty}^{\infty} \left[ (-ik\Omega - in\Omega)^2 [M_n] + (-ik\Omega - in\Omega) [C_n] \right. \\ & \left. + [k_n] \right] \{q_{k+n}\} \quad (5) \\ \text{for } k = & -\infty, \dots, 1, 2, 3, 4 \dots \infty \end{aligned}$$

Here vector  $\{q_k\}$  represents Laplace transform of  $k^{\text{th}}$  component of the deflection vector  $\{q\}$ . In principle, Equations 5 can be used to solve any number of harmonics simultaneously. But in practice, it is sufficient to truncate the summation ( $n = -1, 0, +1$ ) for each value of  $k$ . For example, if aerodynamic transfer matrix corresponding to 4 per rev ( $k=4$ ) response is desired, the blade harmonic motions at 3, 4 and 5 per rev ( $q_3, q_4, q_5$ ) have to be simultaneously computed under this procedure. The error involved is presumed to be small due to the exclusion of higher order interharmonic coupling ( $n>2$ ). Moreover, if desired, once all the desired harmonics ( $N_p$ ) have been computed ( $q_k, k = 1, 2, \dots, N_p$ ) by above

procedure, more accurate airloads can be computed during a final "pass" using Equations 5 for full  $N_p$  values of  $n$ . Thus, an iterative procedure will reduce the error due to the truncation to a minimum. There are a number of additional factors which may make it necessary to follow the iterative procedure in order to obtain more accurate results. These are discussed next.

#### Possible Reasons for Iterative Procedure

1) As mentioned in the previous section, the periodic coefficient matrices involve terms proportional to  $[1-C'(k)]$ , which cannot be conveniently accounted for under the present procedure; unless, of course,  $C'(k)$  is given a constant value. Even though these terms are small, they can be appropriately included if an iterative procedure is followed. During each iteration, vector  $\{q\}$  corresponding to previous iteration can be used and  $[1-C'(k)]$  can be replaced by an indicial form equivalent (for example indicial form of Wagner function, Reference 5, Page 15). Thus, the resulting time-domain forces corresponding to  $[1-C'(k)]$  can be computed and these can be included in the vector  $\{F_{A0}\}$  of the Equations 1.

2) If the elastic deflections of the blade are significantly large, such as large torsional deflections during dynamic stall, the matrices in Equation 1 may be in error due to presence of significant nonlinearities. But, if an iterative procedure is followed, the aerodynamic forces corresponding to large blade elastic deflections (estimated from previous iteration) can be directly included into forcing vector  $\{F_{A0}\}$  of Equation 1. This procedure will minimize the errors due to the nonlinearities.

3) For correct blade dynamic response, it is necessary to use nonuniform induced velocity distribution over the rotor disk. This nonuniform induced velocity distribution is normally computed by using a free-wake analysis (Reference 10, for present analysis), wherein strength of wake vortices depend on blade dynamic response. Thus, deformed free-wake effects on rotor dynamic response can be correctly accounted only by following a solution method which involves iterative procedure that couples the free-wake circulations to the blade motions.

#### Application of New Conventional Unsteady Aerodynamics Model

The existing unsteady aerodynamics model in Reference 1 analysis was found to be highly inaccurate and limited in scope. For example, it assumed the aerodynamic mass matrix  $[M_A]$  in Equation 1 to be equal to zero. A new unsteady aerodynamics model based on current state-of-art was developed and incorporated in the RAVIB analysis (Reference 1). The basic equations utilized were similar to the ones given in Reference 6 (Section 11-8 on Page 596). The effects of radial flow, lift deficiency function, dynamic inflow (optional) were appropriately incorporated in the model. The development essentially involved accurate formulation and programming of the aerodynamic forcing function  $\{F_{A0}\}$  and the matrices  $[M_A]$ ,  $[C_A]$  and  $[k_A]$  (see Equation 1) in the RAVIB analysis. The resulting analysis was utilized to carry out a correlation of computed blade aeroelastic airloads, bending and torsional moments with flight test data with an

objective of establishing the airloads model. During an earlier study (Reference 12), the frequencies and mode shapes obtained from the Reference 1 analysis were compared with those from other independent analyses and the two results compared very well. Thus, the analysis to be utilized for the present study is a validated computer program that is believed to represent dynamics of helicopter blade quite accurately.

#### Application of Analysis

The RAVIB analysis has been used to compute blade airloads, blade bending and torsional moments for the AH1-G helicopter flying in steady state flight conditions. For the AH1-G helicopter, flight test data are readily available (Reference 13) through DATAMAP (Reference 14). Therefore, it was found convenient to use the Reference 13 flight test data for the present correlation study.

The AH1-G blade structural, geometric and aerodynamic characteristics were obtained from References 13 and 15. These blade characteristics may not correspond exactly to the AH1-G helicopter blade used in the flight tests. Because the main objective of the present study was to demonstrate relative improvements in the correlation between test and theory through the use of better unsteady aerodynamics model, an approximate but representative model of the AH-1G blade was considered to be adequate. The blade was modeled by approximately twenty nonuniform elastic segments. The effects of parameters such as control system stiffness, undersling and drive shaft torsional flexibility were appropriately included in the model. The effects of hub impedance and drive system damping were neglected in the present computations.

#### Results with Conventional Unsteady Aerodynamics

The conventional strip theory was used for computation of airloads. The blade was represented by nine nonuniform strips. At the center of each strip (aerodynamic load application point), the nonuniform azimuthal distribution of induced velocities was computed by utilizing a rotor wake analysis (modified version of Reference 10). The computations for the AH-1G helicopter rotor were carried out at two level flight conditions (114 knots and 142 knots) for which the flight test data were available (flight numbers 610 and 614 in Reference 13). The gross weight for both the flight conditions was 8,300 pounds with  $C_T/\sigma = 0.006$ .

A correlation between computed and measured performance parameters is shown in Fig. 2. As the results indicate, the predicted values of shaft horsepower and collective are within five HP and within half a degree respectively of the test values (Fig. 2). For a radial station corresponding to  $r/R = 0.75$ , correlation between calculated and test airloads is shown in Fig. 3a for a representative flight condition (114 knots). Even though there are significant differences between test and theory when the blade is in certain segments (e.g., near  $\psi = 270$ ) of rotor disk, overall correlation between the two is reasonably good. The similar results for the 142 knots flight condition are shown in Fig. 3b.

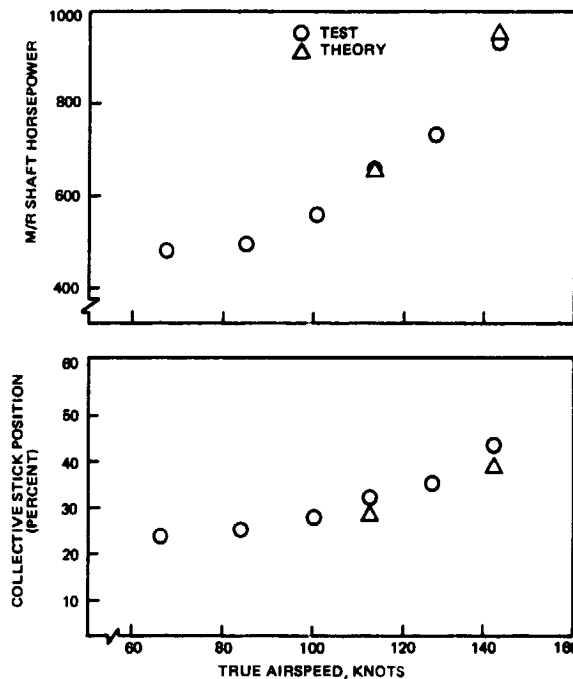


Fig. 2 Comparison of measured and computed level flight performance parameters, AH-1G helicopter, 8300 pounds, GW

Figs. 4a and 4b show the blade oscillatory beamwise bending moment correlation between the test and theory based on the conventional aerodynamics model. For 114 knots flight condition (Fig. 4a) the theory predicts peak to peak value quite accurately, but for 142 knots case (Fig. 4b), the theory underpredicts peak to peak value by 30 percent. Time histories of measured and computed chordwise bending moments for the same flight conditions are compared in Figs. 5a and 5b. From the results shown in these figures, it is seen that very good agreement between test and theory has been obtained over complete range of azimuth.

The correlations of the test blade torsional moments with the predicted results are shown in Figs. 6a and 6b. The peak to peak variation in torsional moment is highly underpredicted by the theory based on conventional aerodynamics model. A thorough analysis of these results indicated that a new aerodynamics model was needed to improve the correlation between computed and test torsional moments.

#### Description of New Unsteady Aerodynamics Model

An analysis of results from two-dimensional experiments (e.g., Reference 16) involving large amplitude oscillations of airfoils (under unstalled conditions) indicates that conventional aerodynamics (based on Theoderson's theory) is unable to predict the unsteady aerodynamic characteristics of the airfoil. This is partly due to the fact that Theoderson's flat plate theory is based on small amplitude oscillations. During high speed forward flight, helicopter blade sections are

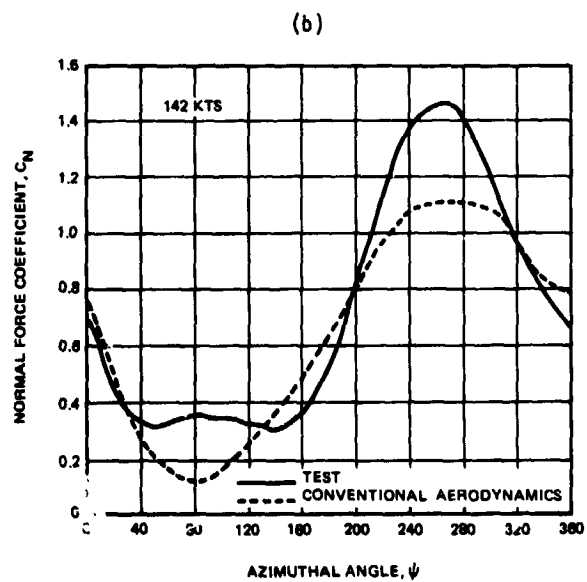
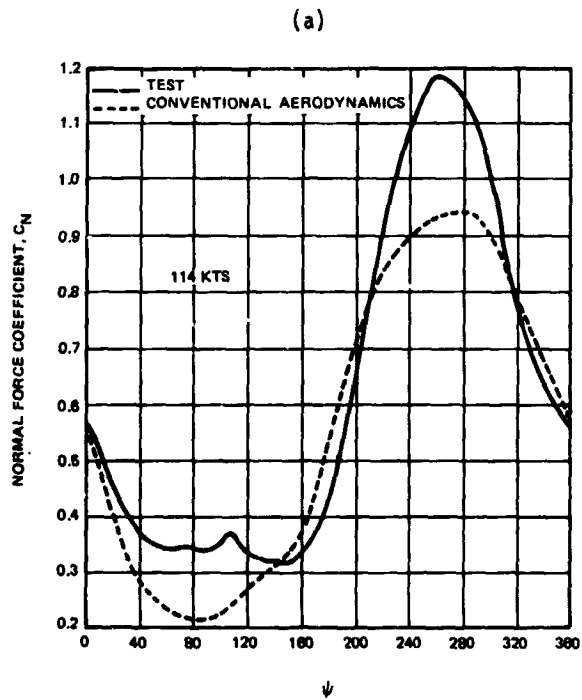


Fig. 3 Correlation between calculated and test airloads, AH-1G Blade,  $r/R = 0.75$

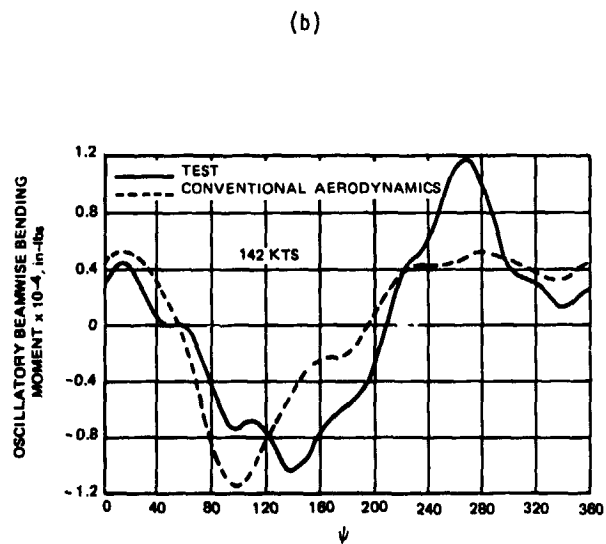
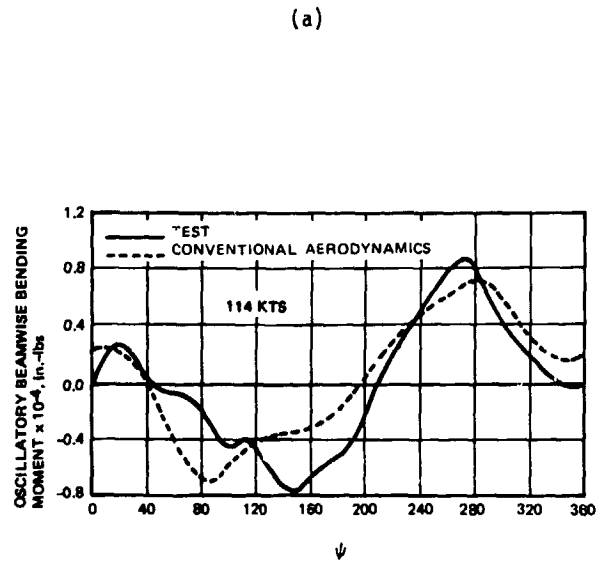


Fig. 4 Comparison between measured and computed oscillator beamwise bending moment,  $r/R = 0.39$ , AH-1G blade

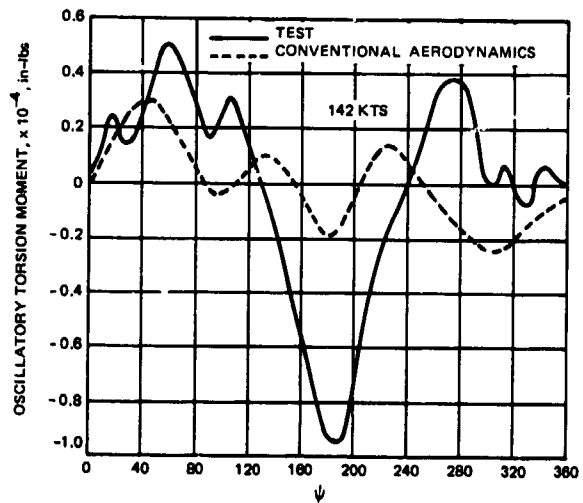
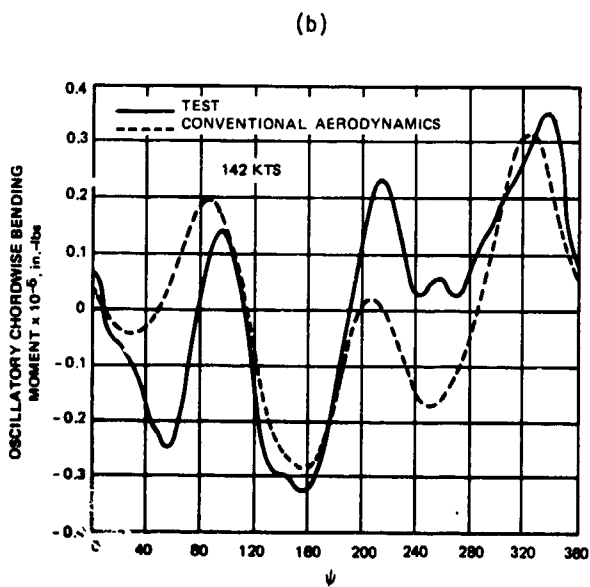
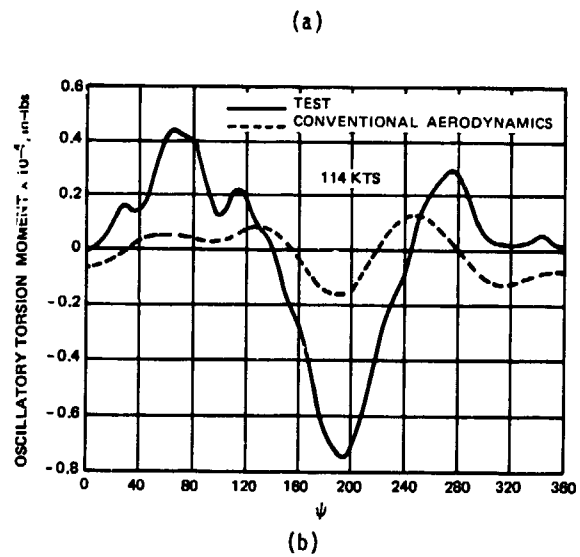
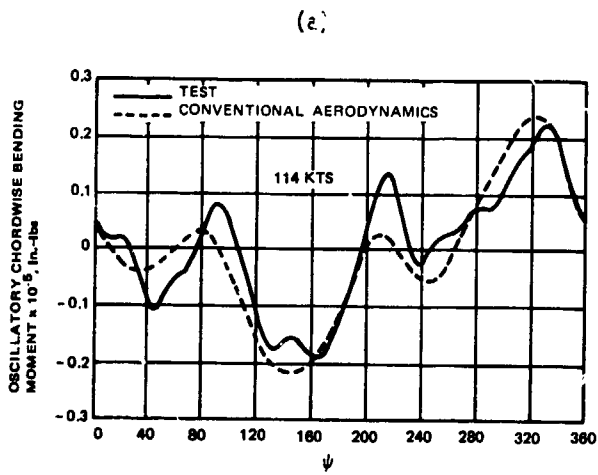


Fig. 5 Comparison between measured and computed oscillatory chordwise bending moment,  $r/R = 0.39$ , AH-1G blade

Fig. 6 Comparison between measured and computed oscillatory torsion moment,  $r/R = 0.30$ , AH-1G blade

expected to go through significantly large amplitude oscillatory changes in angle of attack. Thus, it was found necessary to include the effects of finite amplitude oscillations in the new unsteady aerodynamics model. More specifically, the new unsteady aerodynamics model utilizes empirical or synthesized data. The synthesized data are derived from the test data; by curve-fitting the appropriate analytical expressions to the measured unsteady airfoil characteristics, obtained from the oscillating airfoil experiments. The present method used the analytical expressions established in Reference 5. For example, as described in Reference 5, the unsteady lift coefficient, under uninstalled conditions, is represented by

$$C_{Lu} = C_{Ls}(\alpha) + Q_1 A + Q_2 \alpha_w + Q_3 \alpha + Q_4 \alpha^2 \quad (6)$$

Here  $C_{Ls}$  is the static lift coefficient;  $(A, \alpha_w, \alpha)$  are the instantaneous values of dynamic parameters (see Appendix for details) and  $Q_1, Q_2, Q_3$  and  $Q_4$  are the empirical parameters or the synthesized data. Because the empirical parameters  $Q_1$  through  $Q_4$  are based on real airfoils executing large amplitude oscillations, the Equation 6 correctly simulates general unsteady lift characteristics of a helicopter blade section. Furthermore, it should be noted that lift deficiency function effects are represented in Equation 6 through the decay parameter  $\alpha_w$ , which is derived from a modified Wagner function (Reference 5). In fact, in future, the parameters such as  $Q_1$  through  $Q_4$  can be obtained from some reliable analyses.

Finally, in unsteady aerodynamics the question of what constitutes a large amplitude motion, depends to some extent on the magnitude of the Mach number. An amplitude of one degree in transonic flow is considered high amplitude; whereas at low subsonic Mach numbers, a three degree oscillation may be considered a small amplitude motion. Studies are continuing to establish these criteria.

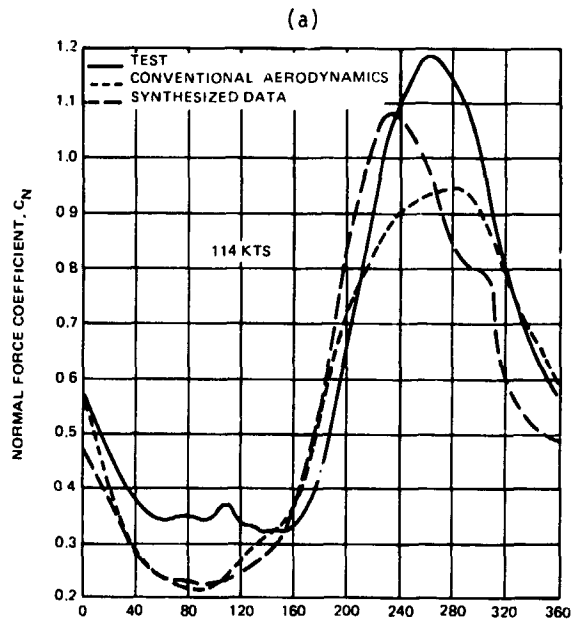
Next, the results based on this synthesized unsteady aerodynamics model are discussed.

#### Results with Synthesized Unsteady Aerodynamics

Equation 6 describes the unsteady lift coefficient,  $C_{Lu}$ , of an airfoil in the time domain. Similar equation for unsteady pitching moment coefficient is given in Reference 5. These two equations were incorporated in the RAVIB analysis. The modified analysis was utilized to recompute the earlier results obtained from the conventional unsteady aerodynamics theory. Thus, the various improvements in the correlation between flight test data and the analytical computations can be systematically demonstrated.

First, the variations in the predicted airloads with aerodynamics model are shown in Figs. 7 through 10. Fig. 7 has been repeated from Fig. 3, but with the addition of computed normal force coefficient based on synthesized data. The differences between the two analytical results are small and these differences are mainly confined to the retreating blade region of the rotor disk. To further illustrate the

closeness of the computed  $C_l$  from the two aerodynamic models, Figs. 8a and 8b show similar results obtained at one more radial station corresponding to  $r/R = 0.86$ . A close analysis of the results, however, indicates a small but significant improvement due to the use of synthesized data, but only for 142 knots flight condition (Figs. 7b and 8b). Thus, improvements in the correlation of beamwise bending moments, if any, can be expected only for 142 knots flight condition. For completeness, Figs. 9 and 10 show the corresponding correlation of chordwise force coefficients for the two radial stations (0.75 and 0.86). Because the results for the chordwise force coefficient from the two aerodynamic models differ only slightly, no significant variations in correlation for the chordwise bending moments is expected with change in the aerodynamics model.



(a)

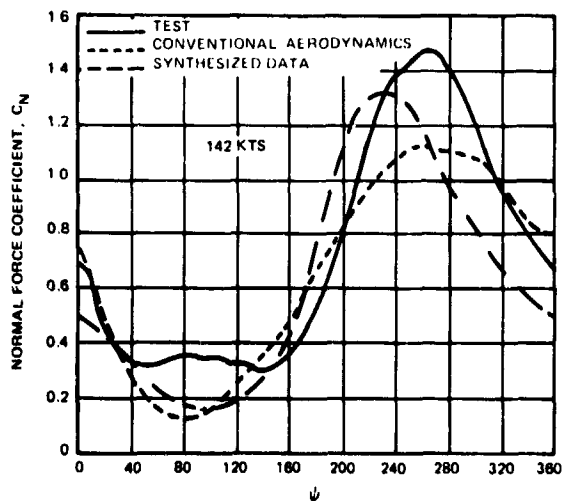


Fig. 7 Correlation between calculated and test airloads, AH-1G blade,  $r/R = 0.75$

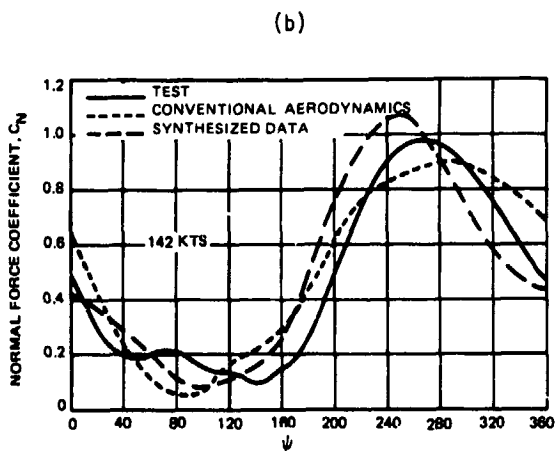
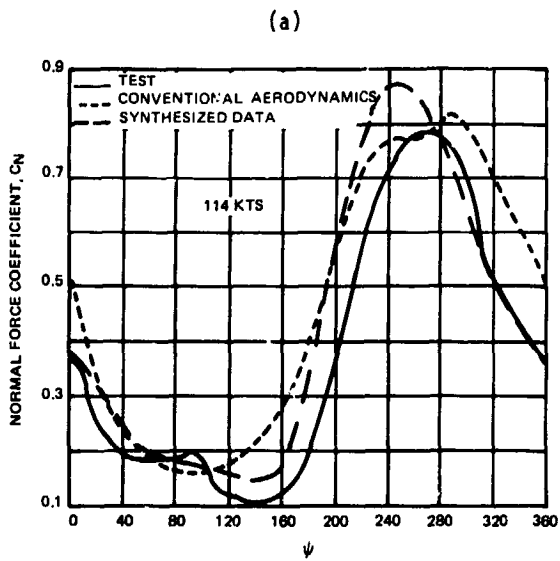


Fig. 8 Correlation between calculated and test airloads, AH-1G blade,  $r/R = 0.864$

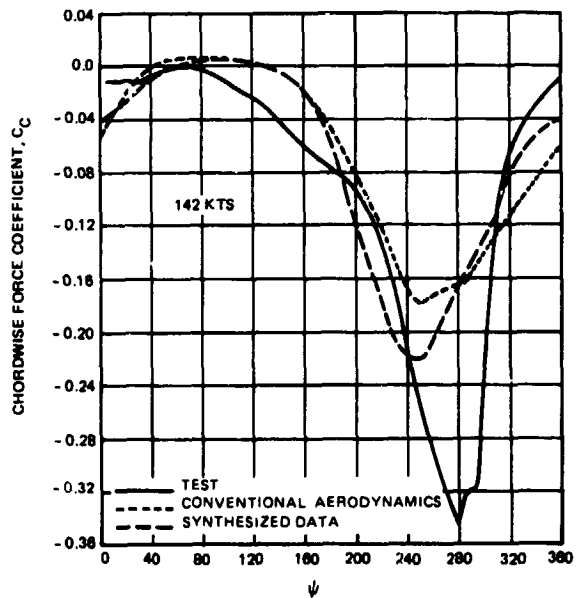
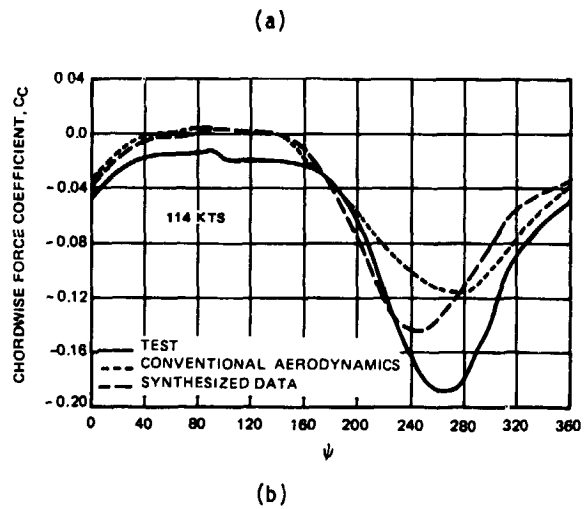


Fig. 9 Correlation between calculated and test airloads, AH-1G blade,  $r/R = 0.75$

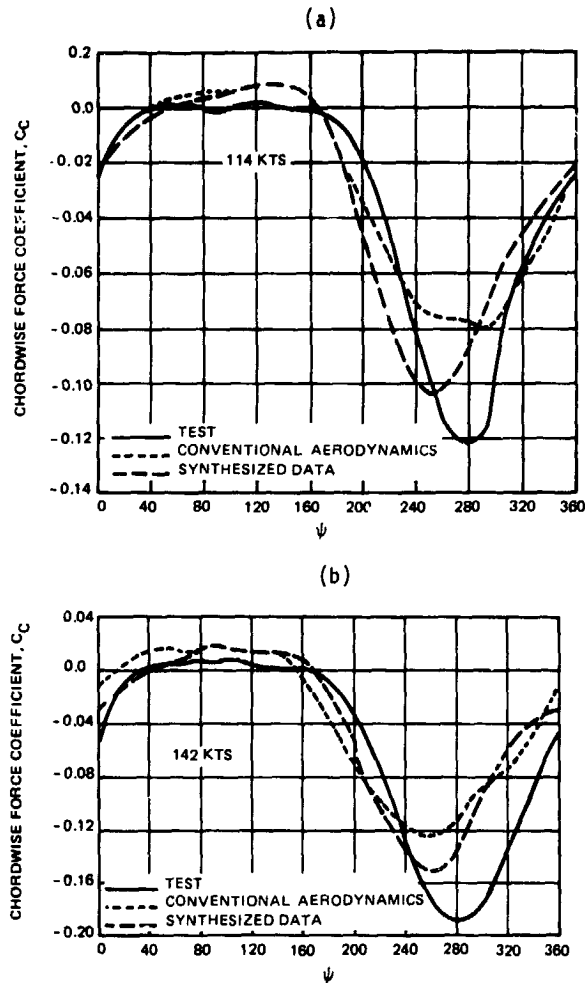


Fig. 10 Correlation between calculated and test airloads, AH-1G blade,  $r/R = 0.864$

Bending Moment Correlations

Figs. 11 and 12 show the comparison between the test and the predicted beamwise bending moment values described for two different radial stations,  $r/R = 0.39$  and  $r/R = 0.80$  respectively. An analysis of these figures indicates the two aerodynamics models predict similar results at 114 knots flight condition (Figs. 11a and 12a). However, at 142 knots flight conditions, the predicted results based on synthesized data (Figs. 11b and 12b) seem to compare better with the test data than those based on conventional aerodynamics.

The similar variation of oscillatory chordwise bending moments for various aerodynamics models are shown in Figs. 13 and 14, corresponding to two radial stations  $r/R = 0.39$  and  $r/R = 0.8$  respectively. Unlike beamwise bending moments, the computed time histories of the chordwise bending moments do not show significant variation with the unsteady aerodynamic model. It should be remembered, however, that the main purpose for developing the present synthesized data model was to improve the correlation between predicted torsional moments and the test data.

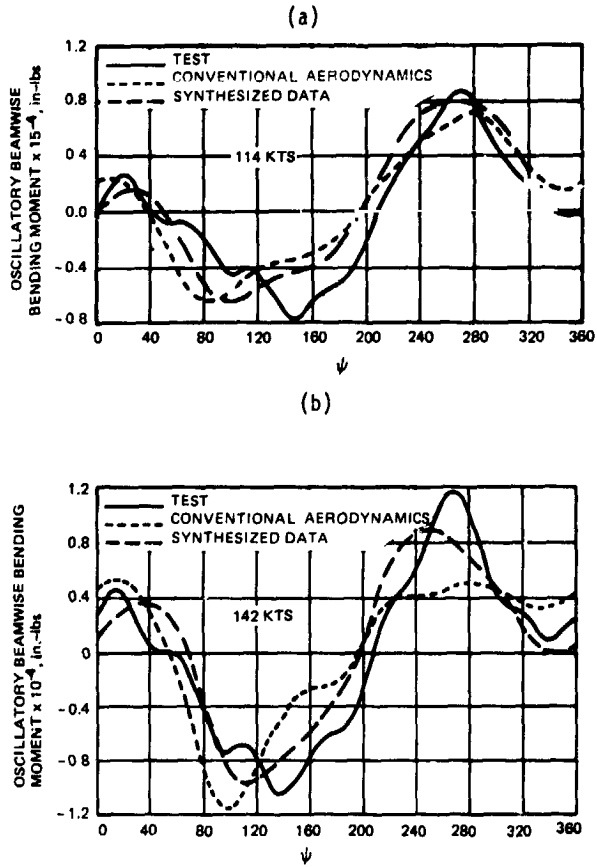


Fig. 11 Comparison between measured and computed oscillatory beamwise bending moment,  $r/R = 0.39$ , AH-1G blade

Torsional Moment Correlation

Measured and computed torsional moments for 114 knots flight condition are compared in Figs. 15a and 16a for two different radial stations,  $r/R = 0.3$  and  $r/R = 0.5$  respectively. From these figures, it is seen that very good agreement between test and new theory based on synthesized data has been obtained over the complete range of azimuth. The computed torsional moments based on conventional aerodynamics do not correlate well with the test data. The similar correlations are obtained at 142 flight conditions as indicated by the results shown in Figs. 15b and 16b. Thus, the results shown in Figs. 15 and 16 imply that for correct computations of pitch link loads, the unsteady aerodynamics model has to be based on large amplitude incidence oscillations inherently encountered by a helicopter blade section.

Finally, it should be mentioned that use of synthesized data will make it easy to extend the airloads computations in the stall region. As established in Reference 5, the unsteady aerodynamics characteristics of blade section during dynamic stall are easily obtained by adding more terms to the right-hand side of Equation 6.

Concluding Remarks

Rotor Aeroelastic Simulation (RAVIS) computer program is a comprehensive, elegant and efficient analysis which seems to predict blade oscillatory loads reasonably well. The conventional unsteady aerodynamics model based on small amplitude airfoil oscillations seem to highly underpredict helicopter blade pitching moments.

Use of a new aerodynamics model based on unstalled synthesized data, derived from the large amplitude oscillating airfoil tests, significantly improves the correlation of the computed blade torsional moments with the test data. Furthermore, this new aerodynamics model is such that it can be easily extended to compute the critical pitch-link loads of a rotor operating under dynamic stall conditions.

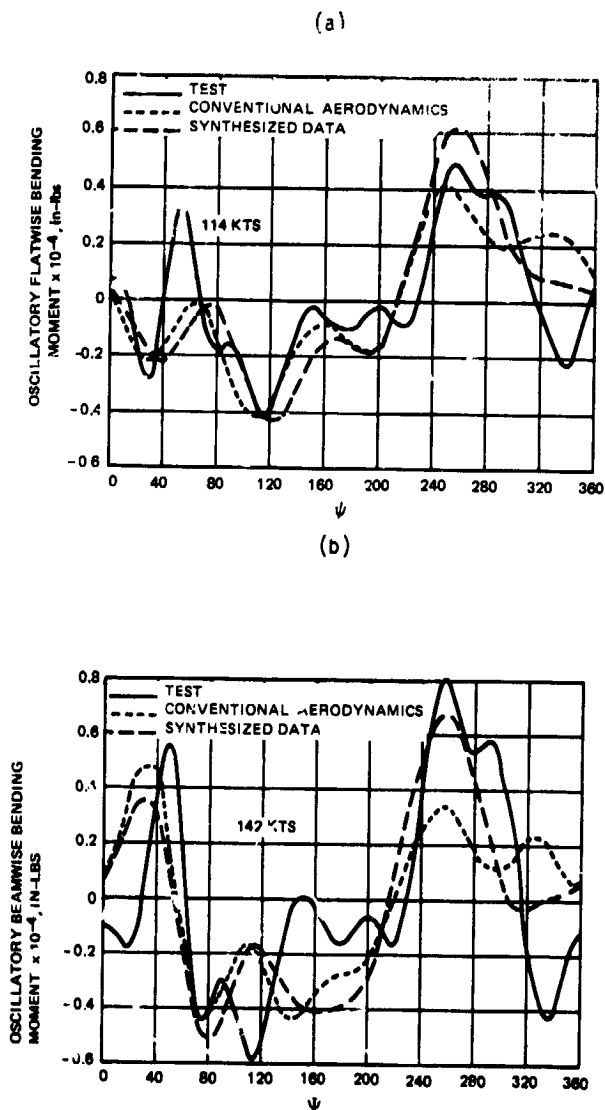


Fig. 12 Comparison between measured and computed oscillatory beamwise bending moment,  $r/R = 0.80$ , AH-1G blade

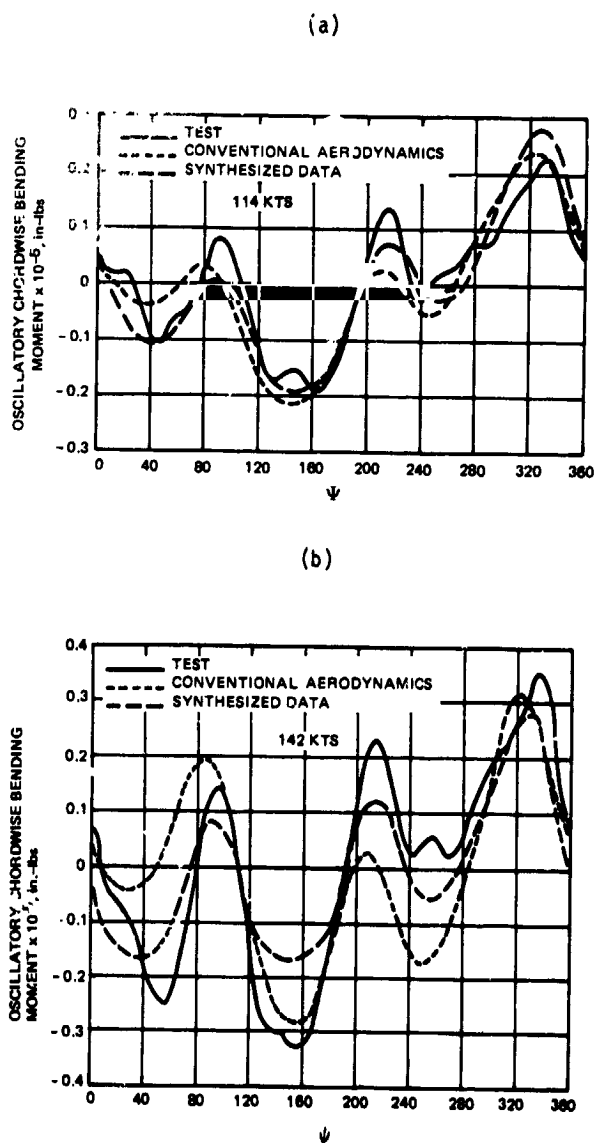


Fig. 13 Comparison between measured and computed oscillatory chordwise bending moment,  $r/R = 0.39$ , AH-1G blade

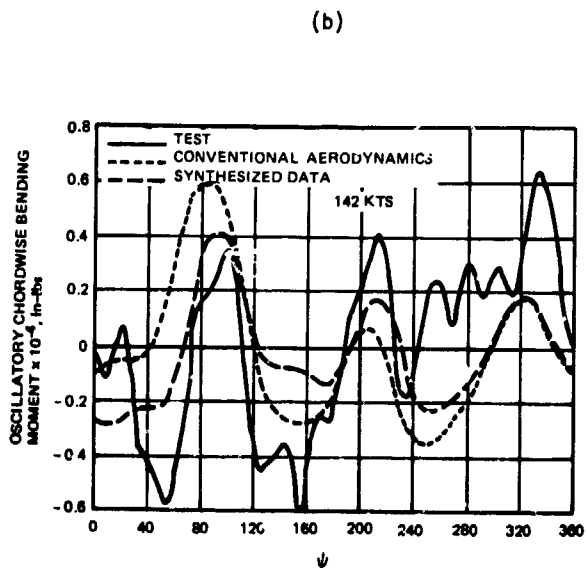
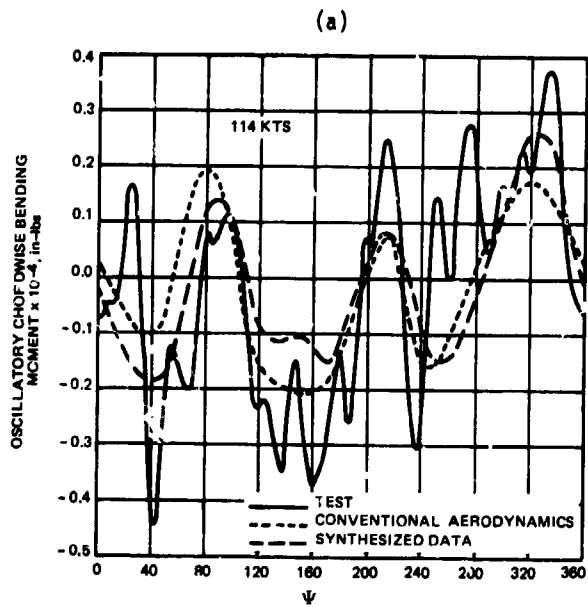


Fig. 14 Comparison between measured and computed oscillatory chordwise bending moment,  $r/R = 0.80$ , AH-1G blade

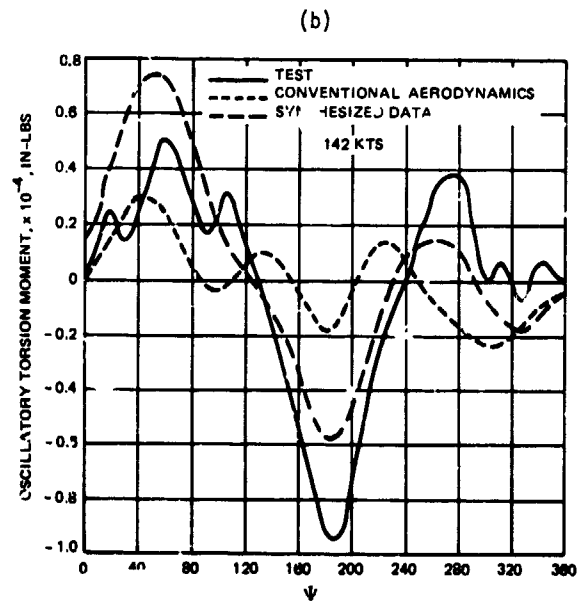
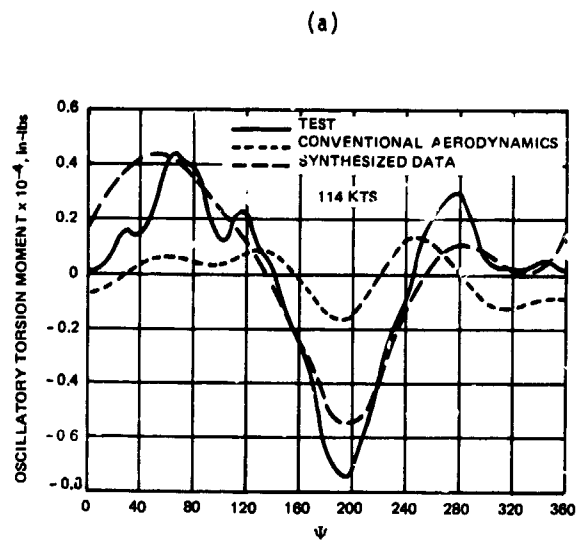


Fig. 15 Comparison between measured and computed oscillatory torsion moment,  $r/R = 0.30$ , AH-1G blade

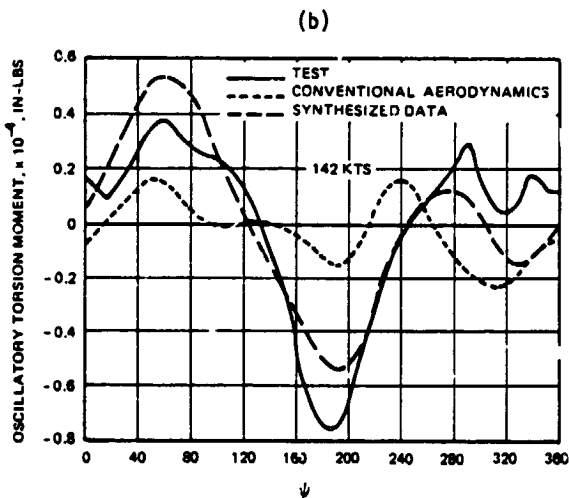
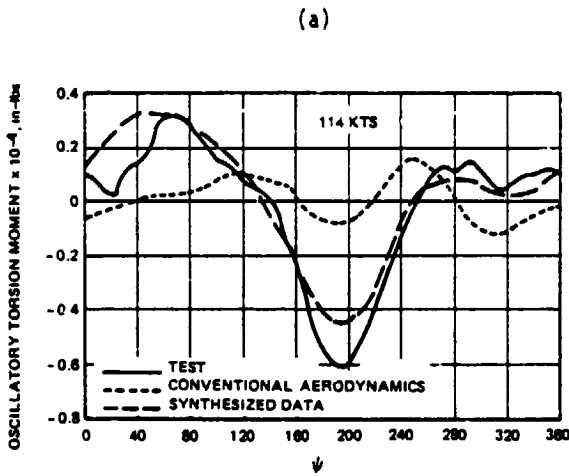


Fig 16 Comparison between measured and computed oscillatory torsion moment,  $r/R = 0.50$ , AH-1G blade

#### APPENDIX

The dynamic parameters utilized in the synthesized data aerodynamics model are: 1) the instantaneous angle of attack,  $\alpha$ ; 2) the nondimensional pitch rate  $A$ ; and 3) the decay parameter  $\alpha_w$ , which accounts for the time history effects of the change in  $\alpha$ , and is based upon the Wagner function.

Because the motion of a helicopter blade is not known a priori, the blade section dynamic parameters are evaluated numerically in a step-wise manner by utilizing the following recursive relationships at step  $n$ .

$$\alpha_n = \theta_n + \phi_n \quad (A-1)$$

$$A_n = (\dot{\alpha})_n / (\Delta s)_n \quad (A-2)$$

$$+ (1.5\phi_n - 2.0\phi_{n-1} + 0.5\phi_{n-2}) / (\Delta s)_n$$

$$(\alpha_w)_n = X_n + Y_n \quad (A-3)$$

where

$$X_n = X_{n-1} e^{-0.0455(1-M^2)(\Delta s)_n} + 0.165 (\alpha_n - \alpha_{n-1}) \quad (A-4)$$

$$Y_n = Y_{n-1} e^{-0.30(1-M^2)(\Delta s)_n} + 0.335 (\alpha_n - \alpha_{n-1}) \quad (A-5)$$

$$(\Delta s) = \frac{2U_n}{\Omega c} (\Delta \psi) \quad (A-6)$$

Here  $\Delta \psi$  is azimuthal stepsize,  $\Omega$  is rotor speed,  $c$  is chord length, and  $U_n$  is tangential velocity component.

The instantaneous angle of attack,  $\alpha_n$ , is described in the tip-path-plane system,  $\theta_n$  and  $\phi_n$  being the pitch angle and inflow angle, respectively. It should be noted that the time derivative of pitch angle in Eq. (A-2),  $(\dot{\alpha})_n$ , may be computed analytically from the known cyclic or harmonic inputs, while the time derivative of  $\phi$  has to be computed by the backward difference scheme. The derivation of Eqs. (A-1 thru A-6) for  $\alpha_w$  is described in Reference 5.

## References

1. Sutton, L.R., and Gangwani S.T., "The Development and Application of an Analysis for the Determination of Coupled Tail Rotor/ Helicopter Air Resonance Behavior", USAAMRDL TR-75-35, Ft. Eustis, VA, August 1975.
2. Dinyavari, M.A.H., and Friedmann P. "Unsteady Aerodynamics in the Time and Frequency Domain for Finite Time Arbitrary Motion of Rotary Wings in Hover and Forward Flight, 25th Structures, Structural Dynamics and Materials Conference, Palm Springs, CA, May 14-16, 1984.
3. Dat, R., and Tran C.T., "Investigation of the Stall Flutter of an Airfoil with a Semi-Empirical Model of 2-D Flow", Vertica, Vol. 7, No. 2, pp. 73-96, 1983.
4. Kaza, K.R., and Kvaternik, R.G., "Nonlinear Aeroelastic Equations for Combined Flapwise Bending, Chordwise Bending, Torsion, and Extension of Twisted Nonuniform Rotor Blades in Forward Flight", NASA TM 74059, August 1977.
5. Gangwani, S.T., "Synthesized Airfoil Data Method for Prediction of Dynamic Stall and Unsteady Airloads", NASA CR-3672, February 1983.
6. Theodersen, T., "General Theory of Aerodynamic Instability and Mechanism of Flutter", NACA Report 496, 1935.
7. Dowell, E.H., "A Simple Method for Converting Frequency-Domain Aerodynamics to the Time Domain", NASA TM 81844, 1980.
8. Johnson, Wayne, "Helicopter Theory", Princeton University Press, 1980.
9. Sutton, L.R., R.P. White, Jr., and R.L. Marker, "Wind Tunnel Evaluation of Aeroelastically Conformable Rotor", USAAVRADCOM TR-81-D-43, March 1982.
10. Sadler, S.G., "Main Rotor Free Wake Geometry Effects on Blade Air Loads and Response for Helicopters in Steady Maneuvers", NASA CR-2110, September 1972.
11. Bisplinghoff, R.L., Ashley, H., and Halfman, R.L., "Aeroelasticity", Addison-Wesley Publishing Company, Inc., Reading, Mass., 1957.
12. Gangwani, S.T., "Evaluation of Helicopter Aeroelastic Stability Analysis", United Technologies Research Center Report Number UTRC82-48, East Hartford, CT, August 1982.
13. Shockey, G.A. and Williamson, J.W., "AH-1G Helicopter Aerodynamic and Structural Loads Survey", USAAMRDL TR-76-39, Ft., Eustis, VA, February 1977.
14. Philbrick, R.G., "The Data for Aeromechanics Test and Analytics - Management and Analysis Package (DATAMAP)", Volume I, USAAVRADCOM - TR-80-D-30A, Ft. Eustis, VA, December 1980.
15. Van Gaasbeck, J.R., "An Investigation of High-G Maneuvers of the AH-1G Helicopter", USAAMRDL-TR-75-18, Ft. Eustis, VA, April 1975.
16. St. Hilaire, A.O., F.O. Carta, M.R. Fink and W.D. Jepson, "The Influence of Sweep on the Aerodynamic Loading on an Oscillating NACA 0012 Airfoil", Volume 1 - Technical Report, NASA CR-3092, 1979.

DISCUSSION  
Paper No. 8

DEVELOPMENT OF AN UNSTEADY AERODYNAMICS MODEL TO IMPROVE CORRELATION  
OF COMPUTED BLADE STRESSES WITH TEST DATA  
Santu T. Gangwani

Jing Yen, Bell Helicopter: I have two questions. Number one: Does your unsteady aerodynamics model include lift, drag, and moment--everything?

Gangwani: The conventional model, you know, it includes only lift coefficient and pitching coefficient, and drag is computed mainly from the lift. In this model you still use the static data and most of the unsteady drag comes from the unsteady lift or from the static drag.

Yen: I know from my experience that the conventional or well-known unsteady aerodynamics model can give you close to good correlation--the moments and everything else, but is very poor in power, and the drag. Your unsteady aerodynamics model here includes everything, including the drag?

Gangwani: I showed you the correlation on horsepower.

Yen: Yes, it was very good.

Gangwani: Edgewise stress correlation is also very good so I don't see any problem in computing the edgewise pulses really.

Yen: My next question is where did your synthesized data come from?

Gangwani: The synthesized data I obtained as I told you from the oscillating airfoil test. Now your question is how did I get [the data] for a particular airfoil?

Yen: That's right.

Gangwani: Well, I sort of took it from other airfoils since your airfoil was a symmetric airfoil. So most of the data corresponds to a [NACA] 0012. It's not an absolute correlation, it's just qualitative to demonstrate that we do need some different aerodynamics models to compute the aerodynamic pitching moments.

Bob Blackwell, Sikorsky Aircraft: I want to ask one question. I wasn't completely clear about whether this model truly handles stall conditions or could it be extended so that it would? The second part of that is were the conditions shown at 142 knots and so forth, at that  $C_T/\sigma$ , did they represent conditions that really would design the control system? In other words were those loads the high loads for the system?

Gangwani: The highest data available are at 142 knots and there was no stall. The stall results that I showed were just computational results at  $C_T/\sigma$  of 0.1. There was no test data at that point. They were just computational data. Most of the test data are at  $C_T/\sigma$  much lower than that.